Large Eddy Simulations of the Summertime Cloudy Boundary Layer Over Arctic Ocean

Q. Zhang, V. Filyushkin and K. Stamnes
Geophysical Institute, University of Alaska
Fairbanks, Alaska

D. Lilly
Cooperative Institute for Mesoscale Meteorological Studies
University of Oklahoma
Norman, Oklahoma

Introduction

Arctic stratus clouds (ASC) are important modulators of global climate. Through interaction with radiation, they have an important influence on the surface fluxes of heat, moisture and momentum in the boundary layer. Due to lack of properly understanding the clouds formation and their interactions with radiation, ASC are currently not realistically simulated by general circulation models (GCMs). This remains one of the main obstacles in improving climate modeling.

ASC are one of the most prevalent features over the Arctic Ocean during the summer season. The low level cloud amounts exceed 70% during the summer months from May through September. ASC may be formed under a wide range of meteorological conditions (Tsay and Jayaweera 1984). The structures of ASC-capped boundary layer are therefore quite complex and variable. They are often observed with strong inversions of temperature and humidity overlying a stable boundary layer. Multiple layers of cloud appear frequently. Such properties greatly complicate ASC modeling.

Model Description

Modeling of ASC during the past years was developed essentially in two main directions. The first makes use of integrating mixed-layer models. The second makes use of one-dimensional ensemble-averaged models. Nevertheless, the complicated features such as the inversions of temperature and humidity, as well as the existence of multiple layers makes it difficult to develop models based on the simplifying assumption of a well mixed boundary layer. Filyushkin and Lilly (1993) proposed to use a 3-dimensional Large Eddy Simulation (LES) approach to study the ASC-capped planetary boundary layer (PBL). The concept of LES is to explicitly simulate the large eddies, which contain most of the energy and dominate turbulent fluxes within the PBL, and to parameterize the subgrid-scale motions, which contain less energy and are less important. With a LES model, Zhang and Filyushkin (1995) successfully simulated two cases of ASC boundary layer.

Large-Eddy Simulation is a useful tool to investigate the turbulence on the boundary layer. Much of the previous work on PBL with LES models have been focused on various aspects of the convective or the neutral boundary layer. In recent years, stably stratified boundary layers have attracted increasing attention. Mason and Derbyshire (1990) simulated a stably stratified PBL and showed the LES was possible. Andren (1995) studied dry stably-stratified PBL by LES with two different subgrid-scale models and showed that an improved subgrid-scale model version (Sullivan et al. 1994) gave improvement in the near-surface region.

The complete set of equations for our LES model have been described in Moeng (1984). Two subgrid-scale models were used. One is an eddy-viscosity model based on a time-evolving turbulent kinetic energy equation. Another is its improved version which was proposed by Schumann (1975) and first used by Sullivan et. al. (1994) to study PBL. A bulk parameterization scheme is used for cloud formation.

The longwave radiation is parameterized according to Herman and Goody (1976). According to the analyses of Tsay et al. (1989), the solar heating was about 10% of the infrared cooling. In order to save the computing time, solar radiative effects were not considered in the following simulations.

Results

Two simulation results were presented in this paper. The initial data were based on the observations of June 28, 1980, during the Arctic Stratus Clouds Experiment. Detailed descriptions of the experiment and analyses of physical properties of the boundary layer were given by Tsay and Jayaweera (1984). Two nearly parallel layers of stratus clouds were observed (Figure 1b). The upper layer of clouds, with its top at near 1200 m and base at 800 m, was capped with a strong temperature inversion and significant moisture decrease. The lower layer of clouds, with its top at about 110 m, formed within a very stable layer near the earth surface. Between the two layers of clouds, a weak stably-stratified layer existed (Figure 1a).

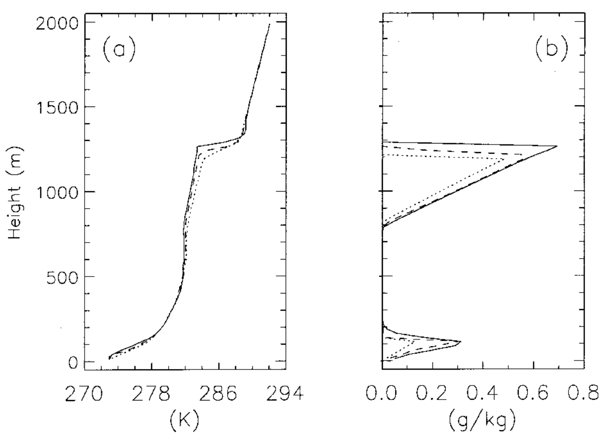

Figure 1. Vertical profiles of (a) potential temperature, and (b) liquid water mixing ratio. Dotted: initial data. Dashed: simulation at 3600 s. Solid: simulation at 7200 s.

Our simulations were made in a horizontal range of 3.2 km x 3.2 km, with a horizontal resolution of 50 m and vertical resolution of 25 m. In order to minimize the effect of gravity waves, a 2 km vertical range was chosen. The results shown below are the simulations at 7200 s.

Simulation I: Structure of ASC-Capped PBL

In this simulation, the old version of the turbulence energy subgrid-scale model was used. The initial data were based primarily on the paper of Tsay and Jayaweera (1984). Two layers of clouds were given (Figure 1b). The ground surface temperature was set to 273.15 K.

The vertical profiles of potential temperature and liquid water mixing ratio are shown in Figure 1. The mean profiles show that the model is able to simulate the complex structure of ASC-capped PBL. The main deficiency in the model was a slight over-estimation of liquid water content in the cloud layers. The simulated liquid water mixing ratio of the upper layer clouds continued to increase, from initial 0.5 g/kg to 0.7 g/kg. The cloud top was also elevated from 1200 m to 1300 m. Correspondingly, the temperature inversion layer lifted about 100 m. Liquid water mixing ratio of the lower layer clouds was also over-estimated. It increased from initial 0.13 g/kg to 3.0 g/kg during the first simulation hour, and maintained stably during the second hour.

The vertical profile of turbulent kinetic energy exhibits two maxima (Figure 2a): the upper maximum near the cloud top is turbulent motions driven mainly by cloud-top cooling; the lower maximum is wind-shear driven. In between, there is a minimum of the TKE, which suggests the decoupling of the two cloud layers in agreement with Curry (1986) and Curry et al. (1988). The large amount of horizontal turbulent kinetic energy (Figure 2b) at the top of the upper cloud layer occurs because the turbulent flow impinges on a very stable layer, and thus the vertical energy component yields to the horizontal component (Moeng, 1986). The vertical TKE exhibits two maxima (Figure 2b). They are, respectively, inside the upper layer clouds where large-scale eddies exist, and right above the upper cloud top due to the trapped gravity waves.

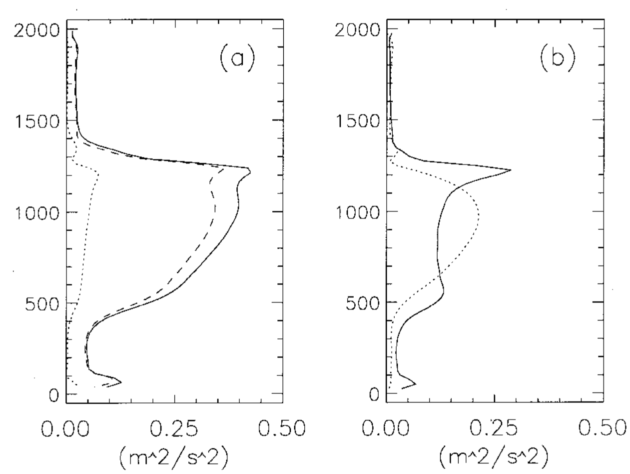

Figure 2. (a) Turbulent kinetic energy (solid: total kinetic energy, dashed: resolved scale, dotted: subgrid scale). (b) Solid: $\frac{1}{2}\left(\overline{u^2}+\overline{v^2}\right)$, dotted: $\frac{1}{2}\overline{w^2}$. Averaged from 3600 s to 7200 s.

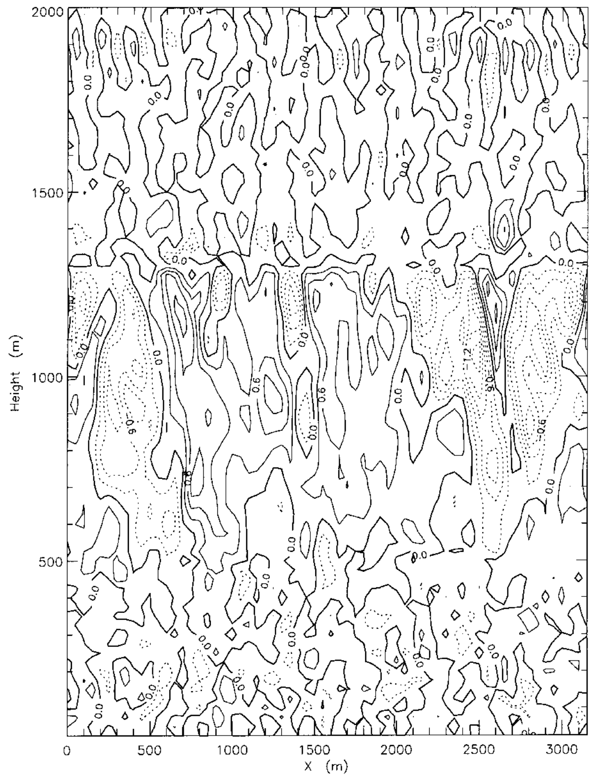

Figure 3. Vertical cross section of vertical velocity w after 7200 second simulation. Unit: m/s. Contours range from -1.5 to 1.2 with an interval of 0.2 m/s. Dotted: w < 0. Solid: w > 0. Heavy: w = 0.

Figure 3 contains a vertical cross section of vertical velocities. The general pattern of eddies also shows that the dynamics in the upper cloud layer are largely decoupled from the lower layer. Several typical eddy scales exist in the different layers. Eddy scales are small around the lower cloud layer and above the top of the upper clouds, where the strong temperature inversion exists. Between the two cloud layers, the well-mixed layer, the motion scales are large.

Temperatures continues to decrease near the upper cloud top (Figure 4a). The maximum averaged cooling rate, with a value of about -3.8 K h^{-1}, exists near the top of upper layer clouds (Figure 4 b). It was caused mainly by the strong radiative cooling of the cloud top (-7 K h^{-1}). The effect of radiative cooling was decreased by the vertical heat transport (Figure 4 d). There existed upward vertical heat flux under the cloud top and downward heat flux right above the cloud top. Both of these two processes transported heat to the cloud top and compensated the cloud top cooling. In nature, the solar radiation also had an effect of decreasing the cloud top cooling.

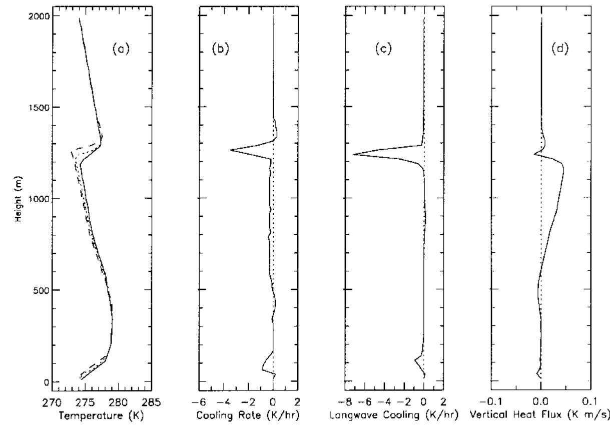

Figure 4. Vertical profiles of (a) temperature (solid: initial data; dashed: at 3600 s; dotted: at 7200 s), (b) averaged cooling rate of 3600 s to 7200 s, (c) longwave cooling averaged from 3600 s to 7200 s, (d) vertical heat flux averaged from 3600 s to 7200 s.

Another maximum cooling rate appeared above the lower layer clouds. Radiative cooling was the main factor. The vertical heat transport also caused the cloud top cooling. A slight downward heat flux existed under the top of the clouds.

Simulation II: Evolution of Clouds

The second simulation is to examine the evolution mechanism of ASC. In this simulation, the initial data set follows that used by Smith and Kao (1996). Initial relative humidity was 85% near the surface, increasing linearly to 100% at 900 m, and was set to 100% between 900 m and 1200 m. From 1200 to 1300 m, the relative humidity decreased linearly from 100% to 85%. It was set to 85% above 1300 m. In order to examine the evolution of clouds, the initial liquid water mixing ratio for the upper layer clouds (Figure 5a) was given only 0.2 g/kg, much smaller than the observation of 0.5 g/kg. No initial cloud was given for the lower layer clouds.

Two subgrid-scale models had been tested and compared. The simulation with the improved version of subgrid-scale model given an improvement on the near-surface layer. Therefore, the results shown bellow were the simulation with the improved version of subgrid-scale model.

After two hours of simulation, the liquid water mixing ratio in the upper layer clouds increased to 0.7 g/kg, comparable to that obtained in simulation I. The clouds developed rapidly in the first simulation hour. Liquid water mixing ratio increased to about 0.5 g/kg at 3000 second, which was

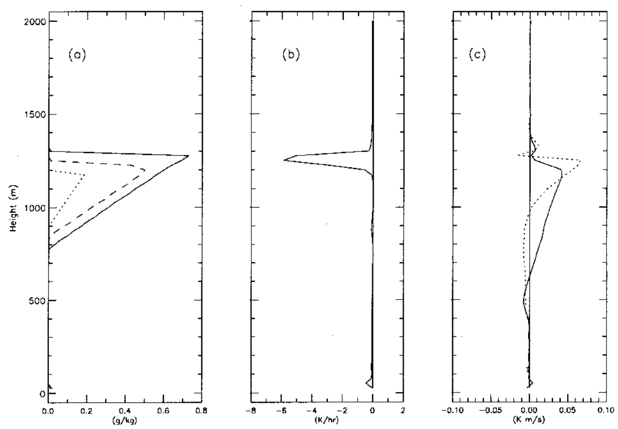

Figure 5. (a) Liquid water mixing ratio. Dotted: initial data. Dashed: simulation results at 3000 second. Solid: simulation at 7200 second. (b) Longwave cooling averaged from 3600 s to 7200 s. (c) Vertical heat flux. Solid: averaged from 3600 s to 7200 s. Dotted: at 7200 s.

comparable with the observation. During the first simulation hour, very strong upward vertical water vapor fluxes (not shown) appeared under the upper cloud layer, implying that the vertical mixing had a significant influence on the first stage of cloud development.

There was also a tendency of formation of a low cloud layer due to cooling of the air to the surface layer. The averaged relative humidity reached 99% near the surface. Some sporadic clouds formed. Vertical heat transport and longwave cooling were the two main processes which caused the formation of the clouds. A slight downward vertical water vapor fluxes existed on the lower layers (not shown).

According to the observation, the clouds formed due to the warm air flowing over the packed ice (Tsay and Jayaweera 1984). In our simulation, the initial temperature near the surface layer was set to 1.2°C, which was very close to the temperature of melting ice. If a higher initial temperature near the surface was given, we might expect more cloud water in the lower layers.

Conclusions

Based on our results, the 3-D LES model is able to simulate reasonably well the case observed on June 28, 1980, although the clouds were slightly over estimated. The evaluation of cloud top may be controlled after introducing the solar radiative effect. In nature, some mechanisms such as precipitation have influence on decreasing cloud evolution. They are not considered in our model.

Our results suggest that the dynamics of the two cloud layers were decoupled and the evolution mechanisms of the two cloud layers were different. After the upper layer clouds initially formed near the peak of the temperature inversion, vertical mixing caused large amount of water vapor transported upward, and thus led to the further development of the clouds. The longwave cooling then increased and had a positive feed back to the cloud development. Vertical heat fluxes had an effect of decreasing the evolution of the upper layer clouds.

Both of vertical heat flux and longwave cooling had effects of increasing the formation of the lower layer clouds.

Acknowledgment

This work was supported by NSF DPP-Polar Ocean & Climate Systems Grant OPP94-15350, by the Department of Energy through contract 091574-A-Q1 to the University of Alaska, and by the Center for Global Change and Arctic System Research under the 1996 Student Research Grant. We would like to thank Chin-Hoh Moeng at NCAR and Peter Q. Olsson at University of Alaska for their valuable discussions.

References

Andren, A., 1995: The structure of stable stratified atmospheric boundary layers: A large-eddy simulation study. *Quart. J. Roy. Meteo. Soc.*, **121**, 961-985.

Curry, J. A., 1986: Interactions among turbulence, radiation and microphysics in arctic stratus clouds. *J. Atmos. Sci.*, **43**(1), 90-106.

Curry, J. A., E. E. Ebert, and G. F. Herman, 1988: Mean and turbulence structure of the summertime Arctic cloudy boundary layer. *Quart. J. Roy. Meteo. Soc.*, **114**, 715-746.

Filyushkin, V. V., and D. K. Lilly, 1993: Application of a 3D delta-eddington radiative transfer model to calculation of solar heating and photolysis rates in a stratocumulus cloud layer. *Atmospheric Radiation*, **2049**, 56-66.

Herman, G. F., and R. Goody, 1976: Formation and persistence of summertime Arctic stratus clouds. *J. Atmos. Sci.*, **33**, 1537-1553.

Mason, P. J., and S. H. Derbyshire, 1990: Large-eddy simulation of the stably-stratified atmospheric boundary layer. *Boundary Layer Meteorol.*, **42**, 117-162.

Moeng, C. H., 1984: A large-eddy simulation model for the study of planetary boundary layer turbulence. *J. Atmos. Sci.*, **13**, 2052-2062.

Moeng, C. H., 1986: Large-eddy simulation of a stratus-topped boundary layer. Part I: Structure and budgets. *J. Atmos. Sci.*, **43**, 2886-2900.

Schumann, U., 1975: Subgrid scale model for finite difference simulation of turbulent flows in plane channels and annuli. *J. Comp. Phys*., **18**, 376-404.

Smith, W. S., and C. Y. J. Kao, 1996: Numerical simulations of observed arctic stratus clouds using a second-order turbulence closure model. *J. of Applied Meteorology*, **35**, 47-59.

Sullivan, P. P., J. C. McWilliams, and Ch.-H. Moeng, 1994: A subgrid-scale model for large eddy simulation of planetary boundary-layer flows. *Boundary Layer Meteorol.*, **71**, 247-276.

Tsay, S. C., and K. Jayaweera, 1984: Physical characteristics of arctic stratus clouds. *J. of Climate and Applied Meteorology*, **23**, 584-596.

Tsay, S. C., K. Stamnes, and K. Jayaweera, 1989: Radiative energy budget in the cloud and hazy arctic. *J. Atmos. Sci.*, **46**, 1002-1018.

Zhang, Qiuqing, and V. V. Filyushkin, 1995: Analysis of arctic stratus experiment `80 cases using a LES model. *EOS Transactions*, 1995 AGU Fall Meeting, San Francisco, A42A-08.